


 Cite this: *RSC Adv.*, 2021, **11**, 19755

## A pH-sensitive, stimuli-responsive, superabsorbent, smart hydrogel from psyllium (*Plantago ovata*) for intelligent drug delivery†

Jaffar Irfan,<sup>a</sup> Muhammad Ajaz Hussain, <sup>\*a</sup> Muhammad Tahir Haseeb,<sup>b</sup> Arshad Ali,<sup>a</sup> Muhammad Farid-ul-Haq,<sup>a</sup> Tahira Tabassum,<sup>c</sup> Syed Zajif Hussain, <sup>d</sup> Irshad Hussain <sup>d</sup> and Muhammad Naeem-ul-Hassan <sup>a</sup>

Herein, we report a polysaccharide-based hydrogel isolated from psyllium husk (a well-known dietary fiber) and evaluated for its swelling properties in deionized water (DW) at different physiological pH values, *i.e.*, 1.2, 6.8 and 7.4. Swelling of psyllium hydrogel (PSH) in DW under the influence of temperature and at different concentrations of NaCl and KCl solutions was also examined. A pH-dependent swelling pattern of PSH was observed following the order DW > pH 7.4 > pH 6.8 > pH 1.2. Stimuli-responsive swelling and deswelling (on-off switching) behavior of PSH was observed in DW and ethanol, DW and normal saline, at pH 7.4 and pH 1.2 environments, respectively. Similar swelling behavior and on-off switching attribute of PSH-containing tablets indicated the unaltered nature of PSH even after compression. Scanning electron micrographs of swollen and then freeze-dried PSH via transverse and longitudinal cross-sections revealed hollow channels with an average pore size of  $6 \pm 2 \mu\text{m}$ . Furthermore, PSH concentration-dependent sustained release of theophylline from tablet formulation was witnessed for >15 h following the non-Fickian diffusion mechanism. Subacute toxicity studies revealed the non-toxic nature of PSH. Therefore, dietary fiber-based material, *i.e.*, PSH could be a valuable pharmaceutical excipient for intelligent and targeted drug delivery.

Received 20th March 2021

Accepted 15th May 2021

DOI: 10.1039/d1ra02219a

[rsc.li/rsc-advances](http://rsc.li/rsc-advances)

## 1. Introduction

A vital contribution of plants and plant-derived materials in human routine life can be witnessed through various food products, textile goods, rubber materials, medicines and pharmaceutical ingredients, *etc.*<sup>1–3</sup> From a medicinal and pharmaceutical point of view, different aerial and underground parts of the plant and isolated constituents are being widely used in various dosage forms.<sup>4,5</sup> Additionally, plants are also a rich source of dietary fibers showing many health benefits.<sup>6–8</sup> Moreover, the seeds of many plants comprise polysaccharides, proteins and fats. Upon soaking the seeds of several plants in water, the seed coat extruded mucilage, which was mainly composed of different polysaccharides.<sup>9,10</sup> Such polysaccharides exhibited high swelling capacity in deionized water and the

buffer of near-neutral pH.<sup>11,12</sup> Interestingly, some polysaccharides also displayed swelling and deswelling (on-off switching) behaviors against various external stimuli, *i.e.*, pH, temperature, electrolyte stress, solvents, *etc.*<sup>13–15</sup> Therefore, naturally occurring plant-derived materials, especially polysaccharides, possessing pH-dependent high swelling capacity have potential applications in the development of targeted/site-specific drug delivery systems.<sup>16,17</sup>

*Plantago ovata* (PO) is a commercially important plant and widely distributed in North Africa, Mediterranean regions and Asia, especially in Pakistan and India.<sup>18</sup> The PO seed husk is one of the most famous dietary fibers commonly known as psyllium (syn: isapgol, ispaghula, sand plantain and spogel), which has a plethora of applications in health, medicine and pharma sectors.<sup>19</sup> Psyllium is being widely used for the treatment of the gastric disorder, constipation,<sup>20</sup> diarrhea,<sup>21</sup> ulcerative colitis,<sup>22</sup> and hypercholesterolemia.<sup>23</sup> One of the most valuable uses of psyllium is noted in lowering the glucose concentration in type-2 diabetic patients.<sup>24</sup> Use of psyllium in lowering the cholesterol and low-density lipoprotein level in hypercholesterolemic adults signify its importance as a healthcare material as well.<sup>25</sup> Moreover, the prebiotic potential of psyllium has now been established in clinical trials.<sup>26</sup> Psyllium extruded mucilage upon soaking in water, which was mainly composed of a polysaccharide and its structure is well understood, *i.e.*,

<sup>a</sup>Institute of Chemistry, University of Sargodha, Sargodha 40100, Pakistan. E-mail: [majaz172@yahoo.com](mailto:majaz172@yahoo.com); Tel: +923468614959

<sup>b</sup>College of Pharmacy, University of Sargodha, Sargodha 40100, Pakistan

<sup>c</sup>Faculty of Medical and Health Sciences, Sargodha Medical College, University of Sargodha, Sargodha 40100, Pakistan

<sup>d</sup>Department of Chemistry and Chemical Engineering, Lahore University of Management Sciences, Lahore Cantt. 54792, Pakistan

† Electronic supplementary information (ESI) available. See DOI: [10.1039/d1ra02219a](https://doi.org/10.1039/d1ra02219a)



arabinoxylan. The arabinoxylan has a branched structure having linear chains of  $\beta$ -1,4-linked D-xylopyranose with branches of  $\alpha$ -L-arabinofuranose.<sup>27</sup> It is also a well-known biomaterial/dietary fiber exhibiting many pharmaceutical, medicinal and biomedical applications.<sup>19,28</sup>

Keeping in view the immense importance of plant-derived biomaterials, *i.e.*, mucilages, we are focused on evaluating psyllium hydrogel (PSH) as a stimulus-responsive material for sustained drug delivery. A lot of research work has been reported on the development and evaluation of crosslinked/grafted (chemically modified) psyllium hydrogel for various biomedical and pharmaceutical applications.<sup>29</sup> However, the physical and pharmaceutical properties of pure or unmodified PSH for potential application as a sustained release or targeted release drug delivery system are not explored yet. Therefore, our interest was to evaluate the swelling capacity of PSH at different temperatures and determine the dynamic swelling properties of PSH at physiological pHs, *i.e.*, 1.2, 6.8 and 7.4, and in deionized water. Additionally, this study addressed the swelling and deswelling (on-off switching) behavior of PSH in the powder form and after its compression into the tablet formulation using theophylline as a model drug in water and ethanol, water and normal saline and buffers of pH 7.4 and 1.2, respectively. We also report on the topography of PSH, especially channeling upon swelling in water using scanning electron microscopy (SEM). For possible applications of this versatile biomaterial in drug delivery applications, the determination of the subacute toxicity studies of PSH was aimed.

## 2. Materials and methods

### 2.1. Materials

Psyllium husk was procured from Marhaba Laboratories Pvt. Ltd., Lahore, Pakistan. Anhydrous theophylline (TP) was purchased from MP Biomedicals, Inc. Solon, Ohio, USA. Potassium dihydrogen phosphate ( $\geq 99.0\%$ ), sodium chloride (NaCl) ( $\geq 99.5\%$ ), potassium chloride (KCl) ( $\geq 99.5\%$ ), acetic acid ( $\geq 99.8\%$ ), hydrochloric acid (37.0%), ethanol ( $\geq 98.0\%$ ) and *n*-hexane ( $\geq 95.0\%$ ) were obtained from Riedel-de Haen, Germany. Sodium hydroxide (NaOH) ( $\geq 98.0\%$ ) was purchased from Merck Chemicals GmbH, Darmstadt, Germany. Micro-crystalline cellulose (Avicel® PH 101) and tragacanth gum were procured from Sigma-Aldrich Co. (St. Louis, MO, USA). All reagents and chemicals were of analytical grade and used as such without further purification. Simulated gastric fluid (SGF) and simulated intestinal fluid (SIF) were prepared as per procedure given in USP 34-NF 29. Deionized water (DW) was used throughout this study.

### 2.2. Methods

#### 2.2.1. Isolation and characterization of psyllium hydrogel.

Psyllium hydrogel (PSH) was isolated using the alkali-extraction method as reported by Saghir *et al.*, 2008 with slight modification.<sup>30</sup> Briefly, Psyllium (100 g) was imbibed in DW for 24 h (psyllium: water; 1 : 50 w/v) and maintained the at pH 12 by adding NaOH solution (2.5% w/v) in the mixture. PSH was

isolated through vacuum filtration. Later, PSH was coagulated by maintaining pH at 3 by using concentrated acetic acid. The PSH obtained was de-fatted with *n*-hexane and thoroughly washed with DW until a constant pH was obtained. Finally, the aqueous suspension of PSH was centrifuged, freeze-dried, milled to get powder form, passed through sieve no. 60 and stored in an airtight container. The yield of PSH was found as 21.25 wt%. PSH was characterized through FTIR analysis and the spectrum was recorded on IR Prestige-21 (Shimadzu, Japan) using the KBr disc method.

**2.2.2. Physical properties and flowability parameters of PSH.** Physical properties of PSH, *i.e.*, moisture content (%), particle size ( $\mu\text{m}$ ), water retention capacity ( $\text{g g}^{-1}$ ) and swelling capacity ( $\text{g g}^{-1}$ ) were examined. Particle size was determined using the dry sieving method as described in USP. In this method, the weighed sample was placed in the top sieve and the nest of sieves was mechanically agitated for 5 min. The weight of the sample retained on each sieve was calculated. The sieve through which 95% of the sample was passed was considered the particle size of the sample. Besides these properties, flowability parameters of PSH were also assessed by determining the angle of repose ( $\theta$ ), bulk density ( $D_b$ ), tapped density ( $D_t$ ), Carr's index ( $C_i$ ) and Hausner ratio ( $H_r$ ) using eqn (1)–(5).<sup>31</sup>

$$\tan \theta = \frac{h}{r} \quad (1)$$

$$D_b = \frac{W}{V_b} \quad (2)$$

$$D_t = \frac{W}{V_t} \quad (3)$$

$$C_i = \left[ 1 - \frac{D_b}{D_t} \right] \times 100 \quad (4)$$

$$H_r = \frac{D_t}{D_b} \quad (5)$$

where  $h$  and  $r$  in eqn (1) represent the height (cm) and radius (cm) of PSH powder heap;  $W$ ,  $V_b$  and  $V_t$  in eqn (2) and (3) are the weight (g) of PSH, and bulk and tapped volume ( $\text{cm}^3$ ) of the sample, respectively.

**2.2.3. pH-responsive dynamic and equilibrium swelling of PSH.** The pH-responsive dynamic and equilibrium swelling properties of PSH were evaluated using the tea-bag method, *i.e.*, a 100 mesh screen.<sup>32,33</sup> Accurately weighed sample of PSH (0.1 g) was placed in each of the four tea bags and soaked in DW and buffer solutions of pH 1.2, 6.8 and 7.4. PSH-filled tea bags were placed in an incubator previously adjusted at room temperature. After periodic time intervals, the tea-bags having swollen PSH were removed from media and weighed after blotting the excess media with filter paper. These tea bags were again placed in their respective media for further swelling. Eqn (6) was employed to determine the swelling capacity of PSH.

$$\text{Swelling capacity } (\text{g g}^{-1}) = \frac{W_s - W_o - W_e}{W_o} \quad (6)$$



where,  $W_s$ ,  $W_o$  and  $W_e$  represent the weight of wet tea-bag having swollen PSH, the weight of dry PSH and weight of empty wet tea-bag, respectively.

Equilibrium swelling of PSH was calculated by immersing the weighed amount of PSH enclosed in the tea-bag for 24 h in DW and then the swelling capacity was calculated using eqn (6). These experiments were repeated three times and mean values were reported.

The temperature-dependent equilibrium swelling of PSH was determined in DW at different temperatures, *i.e.*, 25, 50, 60 and 70 °C for 12 h (see ESI†).

**2.2.4. Swelling kinetics.** The experimental data obtained from the swelling study were used to monitor the rate of absorbency of PSH in each media (DW and pH 1.2, 6.8 and 7.4). For this purpose, the swelling data were fed in eqn (7) and (8) to determine the normalized degree of swelling ( $Q_t$ ) and normalized equilibrium degree of swelling ( $Q_e$ ), respectively.

$$Q_t = \frac{W_s - W_d}{W_d} - \frac{W_t}{W_d} \quad (7)$$

where  $W_s$  is the weight of the swollen PSH at time  $t$ ,  $W_d$  is the initial weight of the dried PSH at time  $t$  and  $W_t$  is the weight of water penetrated into the hydrogel from recipient media, *i.e.*, DW and buffers of pH 1.2, 6.8 and 7.4 at time  $t$ .

$$Q_e = \frac{W_\infty - W_d}{W_d} - \frac{W_e}{W_d} \quad (8)$$

where  $W_\infty$  is the weight of the swollen PSH at time  $t_\infty$ ,  $W_d$  is the initial weight of the dried PSH at time  $t$  and  $W_e$  denote the weight of water retained by PSH, *i.e.*, DW and buffers of pH 1.2, 6.8 and 7.4, when swelling reached at equilibrium in each media at time  $t_\infty$ .

Pre-calculated values of  $Q_t$  and  $Q_e$  were put in the second-order kinetics equation (eqn (9)) and swelling kinetics of PSH were analyzed by plotting a graph between the values of  $t/Q_t$  vs.  $t$ .

$$\frac{t}{Q_t} = \frac{t}{Q_e} - \frac{1}{kQ_e^2} \quad (9)$$

The slope of the line  $1/Q_e$  and intercept  $1/kQ_e$  should be linear if the swelling data followed second-order kinetics.<sup>34,35</sup>

**2.2.5. Saline-responsive swelling of PSH.** Equilibrium swelling behavior of PSH was also determined by soaking the tea-bags having PSH (0.1 g) in 0.1, 0.2, 0.3, 0.4, 0.5, 1, 1.5, 2.0, 2.5, 3.0, 3.5 and 4.0 M solutions of NaCl and KCl, at room temperature for 24 h. Swelling capacity was calculated by adopting the same procedure mentioned in the above section using eqn (6). Experimental procedures were repeated thrice for each solution and mean values were presented.

**2.2.6. pH-responsive swelling/deswelling of PSH.** The pH-responsive swelling and deswelling behavior of PSH was evaluated in the buffer of pH 7.4 and 1.2 and performed at room temperature using an incubator. Accurately weighed PSH (0.1 g) was placed in a tea bag and hung in a beaker having a buffer solution of pH 7.4 (100 mL) for 1 h. After that, the same tea bag was placed in a separate beaker having a buffer solution of pH 1.2 (100 mL) for the next 1 h. The swelling capacity of PSH in

both solutions was measured periodically after every 15 min using eqn (6). The whole process of swelling and deswelling (on-off switching) was repeated for four cycles and each experiment was performed thrice.

#### 2.2.7. Saline-responsive swelling and deswelling of PSH.

The saline-responsive swelling and deswelling behaviors of PSH were evaluated in DW and normal saline. Pre-weighed PSH (0.1 g) was filled in a tea bag and hung in a beaker having DW (100 mL) for 1 h in an incubator adjusted at room temperature. After selected time intervals, the tea bag was removed from the beaker and allowed to drain excess DW, followed by determining the swelling capacity using eqn (6). The same tea bag was hung in a separate beaker having normal saline for 1 h to study the deswelling behavior. Similarly, the swelling capacity was calculated using eqn (6) after selected time intervals. The whole process of swelling and deswelling (on-off switching) was repeated for four cycles and the whole procedure was performed three times to get the mean values.

#### 2.2.8. Solvent responsive swelling and deswelling of PSH.

The solvent responsive swelling and deswelling behavior of PSH were evaluated in DW and ethanol. PSH (0.1 g) was filled in a tea bag and placed in DW for 1 h at room temperature in an incubator. After predetermined time intervals, the tea bag was removed and suspended to trench the excess DW. Swelling capacity was determined using eqn (6). Soon, thereafter, the same tea bag was dipped in ethanol for 1 h. The swelling capacity of PSH was determined using eqn (6). Solvent responsive swelling and deswelling (on-off switching) experiments were repeated for four cycles and the whole procedure was performed thrice.

**2.2.9. Scanning electron microscopy.** A scanning electron microscope (FEI Nova, NanoSEM 450) equipped with Everhart-Thornley detector (ETD) operated at 10 kV was used for the surface morphological analysis of PSH in powder form and also in compressed form as in tablet formulations. Seeking this connection, the dried sample of PSH (0.1 g) was swollen in DW, sonicated for 30 min to remove air bubbles (if any) and freeze-dried. Transverse and longitudinal cross-sections of the freeze-dried PSH were taken using sharp blades. Each sample was mounted on an aluminum stub and dried at 25 °C in a vacuum oven for 24 h before recording SEM images.

**2.2.10. Preparation of tablets.** A model drug (TP) was used to appraise the potential of PSH as sustained-release material for the oral drug delivery system. Tablets containing PSH and TP were prepared by the wet granulation method as described by Muhammad *et al.*, using ingredients mentioned in Table 1.<sup>15</sup> Briefly, PSH, TP and microcrystalline cellulose were mixed

Table 1 Composition (mg per tablet) of PSH tablet formulations

Constituents of formulation	PSTP1	PSTP2	PSTP3
PSH	100	150	200
TP	100	100	100
Microcrystalline cellulose	150	100	50
Tragacanth	50	50	50



thoroughly using a pestle and mortar and passed through the mesh no. 40 to homogenize all ingredients. The resultant dry mixture was then granulated with an aqueous tragacanth solution (10%, w/v). Damp mass was dried at 50 °C in an oven under vacuum and passed through the mesh no. 20 to get uniformed size granules. A rotary press fitted with a 9 mm flat surface punch was used to compress the dried granules at 400 ± 6 mg. Hardness, thickness and friability of the prepared tablets were retained in the range of 6–7 kg cm<sup>-2</sup>, 3.55–3.72 mm and 0.84–0.96%, respectively.

**2.2.11. Dynamic and stimuli-responsive swelling and deswelling of tablets.** The swelling capacity of PSH after compression in tablet form was evaluated in DW for 18 h. Formulation PSTP3 was selected for the determination of dynamic swelling capacity in DW, salt solution-responsive equilibrium-swelling capacity and stimuli-responsive swelling and deswelling behavior of tablets. The experimental procedure for the determination of these parameters was the same as described earlier.

**2.2.12. *In vitro* drug release study and release mechanism.** *In vitro* TP release from PSH-containing tablets was conducted out using USP dissolution apparatus-II in SGF for 2 h and in SIF for 16 h at 50 rpm, maintaining the temperature at 37 ± 0.5 °C. Such conditions can give a better idea of the TP release pattern mimicking the gastrointestinal tract (GIT) pH and transit time. To assess the amount of drug release from tablets, 5 mL of sample was drawn at different time intervals and dissolution media (SGF or SIF) was restocked with freshly prepared media. The withdrawn sample was filtered using a 0.45 µm nylon filter and diluted with respective dissolution media if required. The absorbance of the filtered sample was recorded at 272 nm using a UV-vis spectrophotometer and cumulative drug release was calculated through a calibration curve.

Drug release kinetics were determined using different kinetic models, *i.e.*, zero-order (eqn (10)), first-order (eqn (11)), Hixson–Crowell (eqn (12)) and Higuchi (eqn (13)). The drug release mechanism was described using the Korsmeyer–Peppas model (eqn (14)).<sup>36,37</sup> For the determination of drug-release kinetics and mechanism, *in vitro* drug release studies were performed at pH 6.8 for 24 h using the same procedure as described earlier.

$$Q_t = K_0 t \quad (10)$$

where  $Q_t$  represents the amount of drug release from a tablet in time  $t$  and  $K_0$  represents the rate constant for zero order.

$$\log Q = \log Q_0 - \left( \frac{K_1 t}{2.303} \right) \quad (11)$$

where  $Q_0$  describes the initial amount of drug in the tablet,  $Q$  is the remaining amount of drug to be released,  $K_1$  is the first-order rate constant and  $t$  is the time at which the sample is drawn.

$$Q_0^{\frac{1}{3}} - Q_t^{\frac{1}{3}} = -K_{HC} t \quad (12)$$

where  $Q_0$  is the initial amount of drug released from a tablet,  $Q_t$  is the final amount of drug released from the tablets after time  $t$  and  $K_{HC}$  is the Hixson–Crowell rate constant.

$$Q_t = K_H (t)^{1/2} \quad (13)$$

where,  $Q_t$  denotes the quantity of drug released from the tablets after time  $t$  and  $K_H$  is Higuchi rate constant.

$$\frac{M_t}{M_\infty} = k_p t^n \quad (14)$$

where,  $M_t/M_\infty$  is the fraction of drug released in time  $t$ , whereas,  $k_p$  and  $n$  represent the constant of the Korsmeyer–Peppas model and diffusion exponent, respectively. The value of  $n$  indicates the drug-release mechanism, *i.e.*, if the value of  $n = 0.45$ , then the drug release mechanism follows the Fickian diffusion,  $n$  is in the range from 0.45–0.89 and  $> 0.89$ , then it follows non-Fickian diffusion and super case-II transport, respectively.<sup>37,38</sup>

**2.2.13. Subacute toxicity studies.** Subacute toxicity studies of PSH were conducted according to the OECD (Organization for Economic Co-operation and Development)-Guidelines 407 and National Institutes of Health guide for the care and use of laboratory animals (NIH Publications No. 8023, revised 1978).<sup>39</sup> Adult male and nulliparous female Wistar rats (10–12 weeks, 200–250 g) were selected for the study and received from the animal house of the University of Lahore, Lahore, Pakistan. The animals were kept in clean cages under a controlled temperature (22–24 °C), humidity (50%) and 12 h light–dark cycle with free access to standard laboratory diet and water. The animals were divided into four groups ( $n = 10$  in each group, five males and five female), including a control group (not received PSH) and given three doses of PSH (125 mg per kg body weight (bw), 250 mg per kg (bw) and 500 mg per kg (bw)) daily for a period of 28 consecutive days.<sup>40</sup> The experimental protocols were approved by the Institutional Research Ethics Committee of The University of Lahore vide letter no. IREC-2018-76-M, dated May 17, 2018.

During subacute toxicity studies, body weight and food and water consumption were recorded on a daily basis. Moreover, animals were also monitored for any possible signs of toxicity along with symptoms of allergy, diarrhea, change in reflexes, tremors and salivation. At the end of 28 days, all animals were anesthetized and blood samples were collected by cardiac puncture for biochemical and hematological analysis, such as complete blood count, lipid profile, liver function tests, uric acid and renal function tests. Vital organs such as the kidney, heart, spleen, lungs, liver and GIT were removed and weighed for the calculation of absolute organ weight.

Histological analysis was performed to analyze the tissue integrity of vital organs, therefore, important parameters, *i.e.*, degeneration, leukocyte infiltration, necrosis, congestion, apoptosis, fibrosis and extravasation of blood were observed.<sup>41</sup> Vital organs were preserved in 10% buffered formalin. Tissues of vital organs were sectioned at 5 µm thickness and stained with hematoxylin–eosin dye and examined under a light microscope.

**2.2.14. Statistical analysis.** The results of both control and treated groups were expressed as the mean ± standard error of



the mean (SEM). The difference between groups of rats was analyzed through one-way analysis of variance (ANOVA) followed by Dunnett's test. Differences were considered statistically significant at  $p < 0.05$ .

### 3. Results and discussion

#### 3.1. Characterization of PSH

Isolated PSH was characterized using FTIR spectroscopy (Fig. 1). The absorption bands in the FTIR spectrum of PSH were compared with the reported values for similar materials.<sup>42</sup> The assignments of the scrutinized absorption bands were observed at  $3458.37\text{ cm}^{-1}$  (OH stretching as a broad band),  $2962.66\text{ cm}^{-1}$  (aliphatic saturated  $-\text{CH}$  stretching),  $1610.58\text{ cm}^{-1}$  (deformation due to absorbed  $\text{H}_2\text{O}$ ),  $1448.54\text{ cm}^{-1}$  ( $-\text{CH}_2$ ),  $1344.38\text{ cm}^{-1}$  ( $-\text{CH}$ ),  $1076.28\text{ cm}^{-1}$  ( $-\text{C}-\text{C}$ ,  $-\text{C}-\text{O}$ ,  $-\text{C}-\text{O}-\text{H}$  strongly influenced by branching) and a sharp band at  $881.47\text{ cm}^{-1}$  (glycosidic bond, antisymmetric out-of-plane). The absence of absorption bands at  $1650$  and  $1550\text{ cm}^{-1}$ , and  $1520\text{ cm}^{-1}$  representing  $-\text{NHCO}-$  of protein units and ferulic acid, respectively, confirmed that the isolated PSH was free from any such impurities.

#### 3.2. Physical properties and flow-ability parameters of PSH

Results of physical properties and flow-ability parameters of PSH are depicted in Table 2. The values of the angle of repose, Carr's index and Hausner ratio are placed in a category of "poor" flow properties as mentioned in USP. Therefore, before designing the PSH-based tablet formulations, some necessary measurements, *i.e.*, the addition of a lubricant or glidant, selecting the proper binder and its appropriate concentration, and the use of wet/dry granulation method should be taken.

#### 3.3. pH-responsive dynamic and equilibrium swelling of PSH

The pH-responsive dynamic and equilibrium swelling behavior of PSH were evaluated at different pH of GIT using buffers of pH 1.2 (gastric), 6.8 (small intestine) and 7.4 (large intestine), and

Table 2 Physical properties and flow-ability parameters of PSH powder

Flow-ability parameters	PSH
Moisture content (%)	$7.4 \pm 0.4$
Particle size ( $\mu\text{m}$ )	$\approx 250$
Angle of repose ( $\theta$ )	$45.74 \pm 0.25$
Bulk density ( $\text{g mL}^{-1}$ )	$0.495 \pm 0.03$
Tapped density ( $\text{g mL}^{-1}$ )	$0.707 \pm 0.02$
Carr's index (%)	$29.98 \pm 1.76$
Hausner ratio	$1.428 \pm 0.075$
Swelling capacity on 24 h ( $\text{g g}^{-1}$ )	$48.77 \pm 1.2$

in DW (Fig. 2a and c). It was observed that PSH markedly swollen in DW as well as at pH 7.4 and 6.8. However, less swelling was observed in an acidic environment of pH 1.2. In an acidic environment, the carboxylate ion ( $-\text{COO}^-$ ) present in the polymeric networks of PSH, gets protonated and is converted into a carboxylic acid ( $-\text{COOH}$ ). Whereas, in a basic environment, the ionization of the carboxylic acid group ( $-\text{COOH}$ ) takes place causing anion-anion repulsion, which results in increased swelling. Moreover, less swelling at pH 6.8 and 7.4 than DW is due to the charge screening effect offered by an excess of  $\text{Na}^+$  ions. Therefore, being pH-responsive, it could be established that PSH is a valuable candidate for colon-targeted drug delivery systems. Equilibrium swelling also expressed the maximum swelling capacity of PSH in different swelling media.

The swelling of PSH was also compared to already reported swellable polysaccharides.<sup>43–46</sup> After 6 h study in DW, the swelling capacity of PSH was almost similar to the swelling capacity of arabinoxylan containing mucilages, *i.e.*, linseed (*Linum usitatissimum*) hydrogel (LSH) and *Mimosa pudica* seed hydrogel (MPH) (Fig. 2d).<sup>43,44</sup>

The results of temperature-dependent swelling studies revealed that the swelling of PSH is directly proportional to the temperature, *i.e.*, increased with the increase in temperature (Fig. S1, see ESI†).

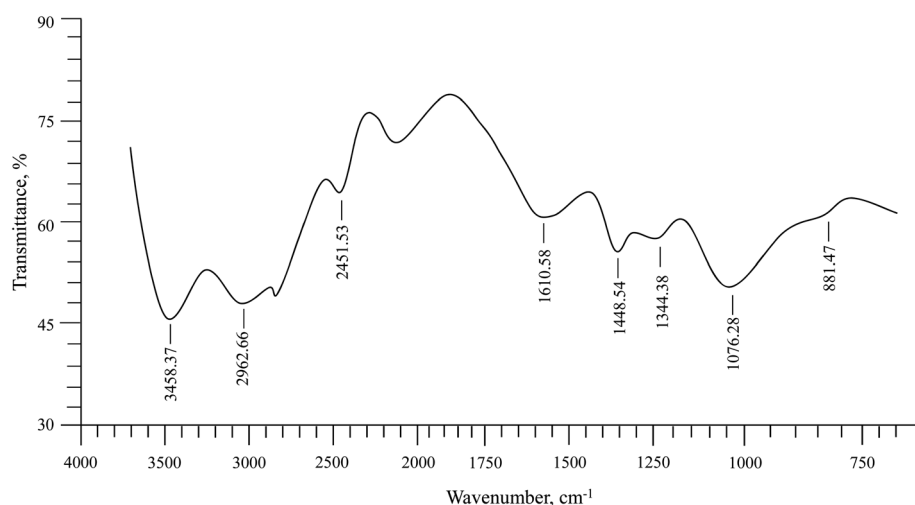


Fig. 1 FTIR (KBr) spectrum of PSH.



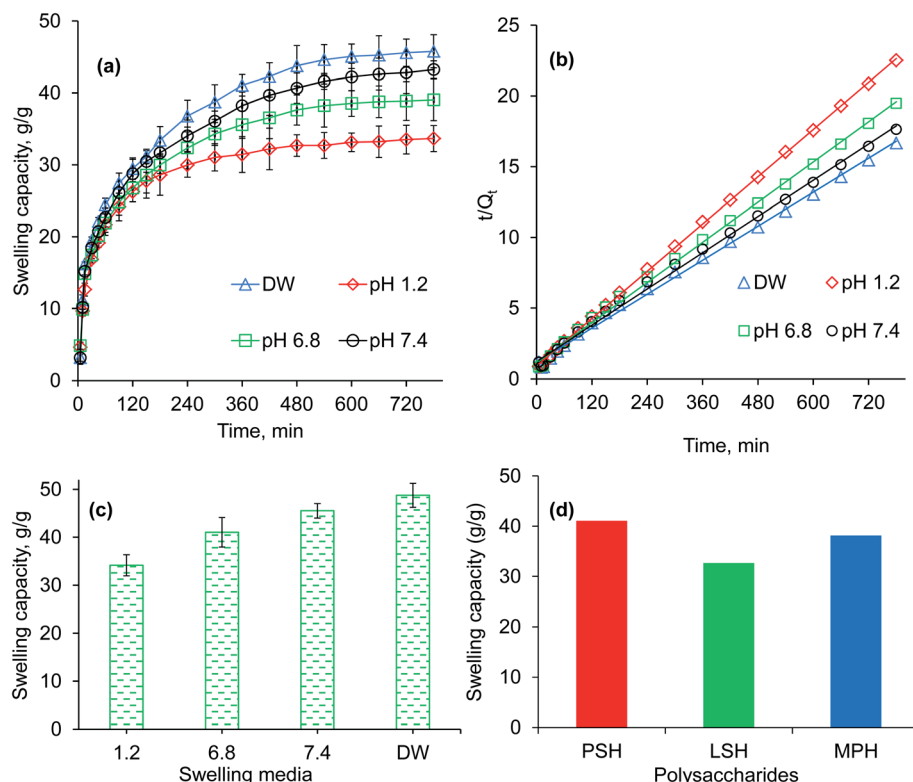


Fig. 2 Swelling capacity (a), swelling kinetics (b) and equilibrium-swelling capacity (c) of PSH powder at pH 1.2, 6.8 and 7.4, and deionized water (DW). Comparison of swelling capacity ( $\text{g g}^{-1}$ ) of PSH with already reported swellable polysaccharides, *i.e.*, LSH (linseed hydrogel)<sup>43</sup> and MPH (*Mimosa pudica* hydrogel),<sup>44</sup> after 6 h study in DW.

### 3.4. Swelling kinetics of PSH

A higher swelling rate with higher swelling capacity is demanding and one of the necessary prerequisites for the practical implication of any hydrogel in formulation design. Therefore, owing to many advantageous applications of hydrogels, swelling kinetics of PSH were studied. As the plot between the values of  $t/Q_t$  (along dependent-axis) and  $t$  (along independent-axis) gives a straight line with a higher value of the regression coefficient ( $R^2 > 0.99$ ), therefore, second-order kinetics were found the best fit for experimental swelling capacity data obtained in DW and at different physiological pH (1.2, 6.8 and 7.4) (Fig. 2b).

### 3.5. Saline-responsive equilibrium swelling of PSH

Saline-responsive equilibrium swelling of PSH is depicted in Fig. 3a. An inverse trend in swelling was observed, *i.e.*, by increasing the concentration of salt solutions, the ability of PSH to swell decreased. At a high concentration of salts in the medium, the number of positively charged ions ( $\text{Na}^+$  and  $\text{K}^+$ ) increases over counter carboxylate ions ( $\text{COO}^-$ ) of PSH that make the penetration of swelling media to PSH difficult. Furthermore, the charge screening effect also minimized the anion-anion repulsion resulting in reduced swelling of PSH. The swelling capacity of PSH in the KCl solution was less as compared with the NaCl solution. Owing to the high charge density of  $\text{K}^+$  ions as compared with  $\text{Na}^+$  ions, the attraction of  $\text{K}^+$  ions toward  $\text{COO}^-$  ions (present on the surface of PSH) is

greater. Therefore, PSH swells less in KCl solution than with NaCl at the same concentration. Our results are in good agreement with the work of peers.<sup>47</sup>

### 3.6. Swelling and deswelling of PSH in water and ethanol

The swelling and deswelling behavior of PSH was evaluated in a water/ethanol environment using the gravimetric method. Due to the greater polarity and dielectric constant of water (80.40) compared with ethanol (24.55), PSH forms strong hydrogen bonding with water and swells. Whereas, on the immersion of swollen PSH in ethanol, rapid deswelling of the PSH was observed owing to the lower polarity and dielectric constant of ethanol. Moreover, ethanol has a greater tendency to replace water molecules and water can escape out from the swollen hydrogel, resulting in the decrease of PSH swelling.<sup>48</sup> Four successive cycles of swelling and deswelling were recorded as depicted in Fig. 3b. Therefore, these findings are directed to conclude that the presence of alcohols may alter the drug release pattern from the drug delivery system. Hence, patients should be advised to avoid concomitant administration of alcohols with any drug delivery system having PSH as an excipient/release retarding agent throughout the treatment of ailments.

### 3.7. Swelling and deswelling behavior of PSH in DW and NaCl

PSH showed swelling in DW and deswelling in an aqueous solution of NaCl (0.9%) (Fig. 3c). In the presence of NaCl



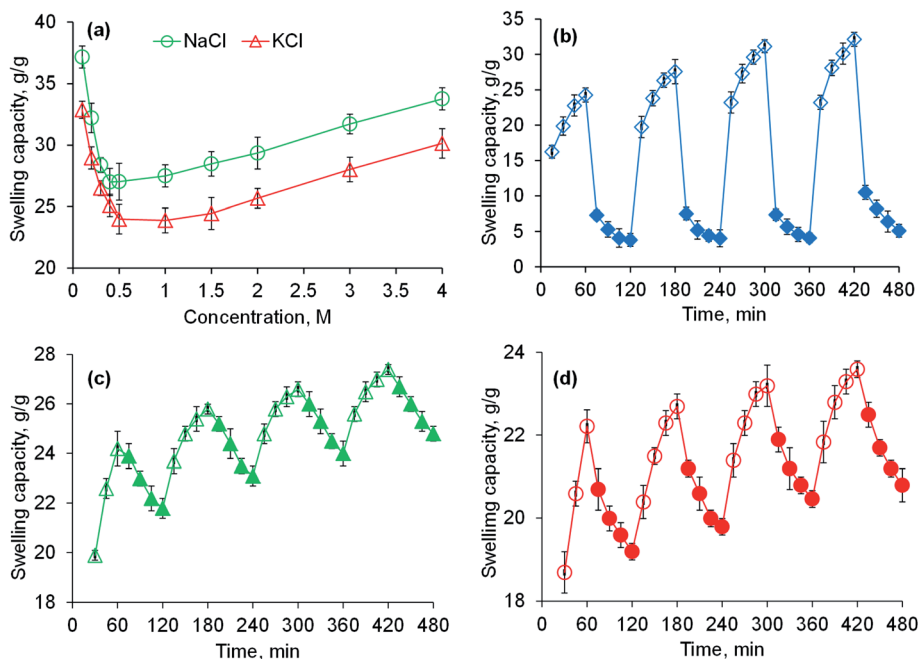


Fig. 3 Swelling capacity of PSH powder in an aqueous solution of NaCl and KCl (a) and swelling and deswelling of PSH powder in DW and ethanol (b), DW and normal saline (c) and pH 7.4 and pH 1.2 environments (d). Empty and filled symbols in (b–d) are indicating the swelling and deswelling phases of PSH powder, respectively.

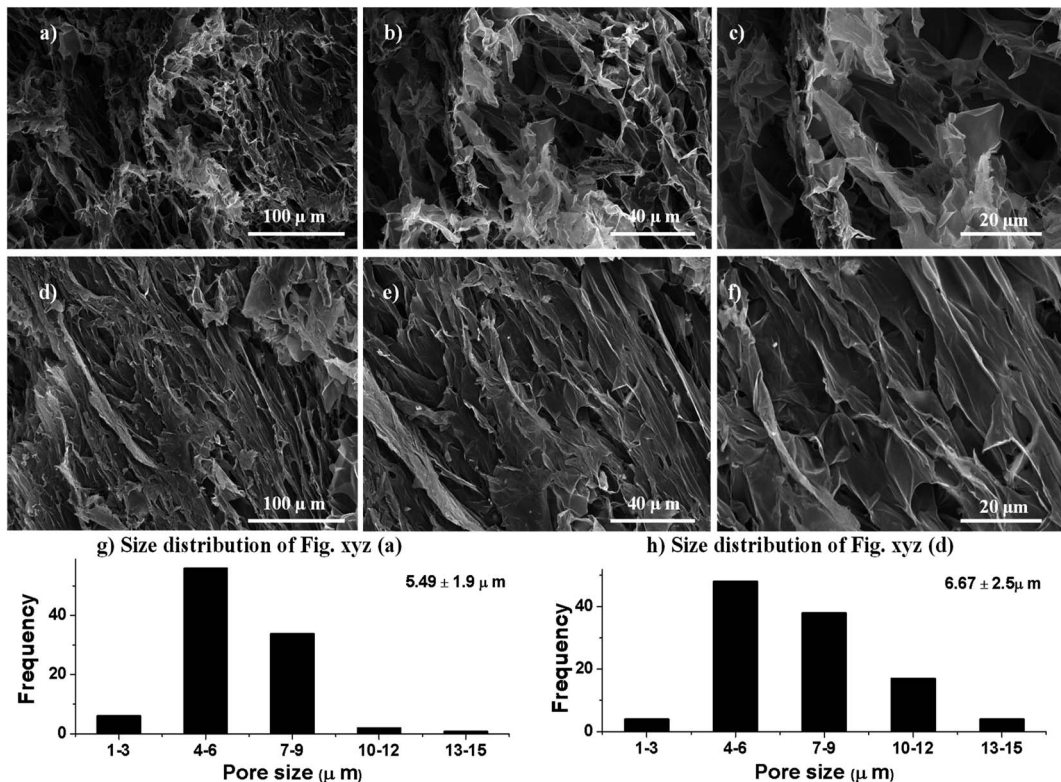


Fig. 4 Scanning electron micrographs of transverse (a–c) and longitudinal (d–f) cross-sections of swollen then freeze-dried PSH (average pore size  $6 \pm 2 \mu\text{m}$ ) at different magnifications. The size distribution of macropores (g and h) of transverse (a) and longitudinal (d) cross-sections.



solution, the concentration of  $\text{Na}^+$  ions increases, which creates the osmotic pressure difference between the swollen PSH and surrounding media.<sup>49</sup> Consequently, water molecules are swept out from swollen PSH and deswelling was observed.

### 3.8. Swelling and deswelling behavior of PSH at pH 7.4 and pH 1.2

To determine the pH-sensitivity of PSH, its swelling and deswelling behavior were evaluated by soaking a precise amount of PSH under pH 7.4 and pH 1.2 environments, respectively. It was observed that PSH swells and deswells in pH 7.4 and pH 1.2 environments, respectively. This study was repeated for four cycles and an almost similar trend of swelling and deswelling was observed as depicted in Fig. 3d. The swelling and deswelling behavior of the PSH follows a similar mechanism as described in Section 3.3.

### 3.9. Surface morphological analysis by scanning electron microscopy

To observe the texture and internal structure of PSH, the morphological analysis *via* transverse and longitudinal cross-sections of swollen then freeze-dried PSH was performed using SEM. It is obvious from the SEM-micrographs of PSH that the surface has wide networking of elongated channels, which are distributed uniformly (Fig. 4). These interconnected channels on the surface of PSH exhibited the average pore size of  $6 \pm 2 \mu\text{m}$ . Owing to these pores or channels, PSH can hold a high amount of water and other solvents. Hence, PSH may be used in cosmetics, diapers, sustained-release drug delivery systems and other pharmaceuticals.

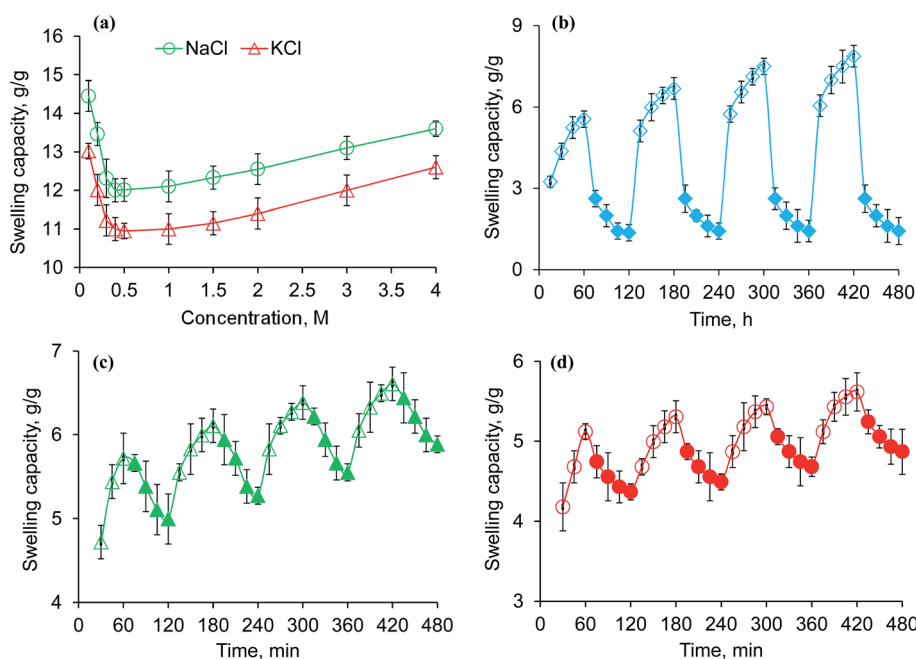


Fig. 5 Swelling capacity of PSTP3 in NaCl and KCl (a), swelling and deswelling of PSTP3 in DW and ethanol (b), DW and normal saline (c) and pH 7.4 and 1.2 environments (d). Empty and filled symbols in (b-d) are representing the swelling and deswelling duration of PSTP3 tablets, respectively.

### 3.10. Electrolyte responsiveness, stimuli-responsive swelling and deswelling, and dynamic swelling of PSH tablets

The investigation of the effect of salt solutions on the swelling capacity of PSH tablet formulation (PSTP3) is depicted in Fig. 5a. A similar swelling trend of these tablets was observed as of PSH powder. However, the swelling capacity of PSH tablets (Fig. 5a) was much less compared powder form (Fig. 3a), mainly due to the compression of PSH. Moreover, inter-particles spaces in tablet form are significantly lower than in powder form, therefore, penetration of swelling media through these tight junctions is difficult. Hence, less swelling was observed in PSH tablets compared with PSH powder.

A significant decline in swelling and deswelling behavior of PSH tablet (PSTP3) compared with PSH powder was observed and expressed in Fig. 5b-d. However, the analogous stimuli responsiveness of PSTP3 tablets to PSH powder in different solvents, *i.e.*, DW and ethanol, DW and normal saline and buffer of pH 7.4 and 1.2 showed that compression of PSH powder in tablet form reduced the swelling capacity.

The swelling behavior of all three formulations (PSTP1, PSTP2 and PSTP3) was studied in DW and results are shown in Fig. 6a. The results illustrated that the swelling of the tablet is directly proportional to the concentration of PSH in the tablet. Moreover, due to compression, the particles of PSH are closely packed and offer a hindrance to swelling media to penetrate. As a result, in tablet form, PSH showed less swelling compared with powdered form. Fig. 6b showed the photographs of aerial and axial views of the tablet during swelling.

### 3.11. *In vitro* drug release studies

The release of any drug from a water-swellable polymeric matrix usually starts with the penetration of dissolution media into the



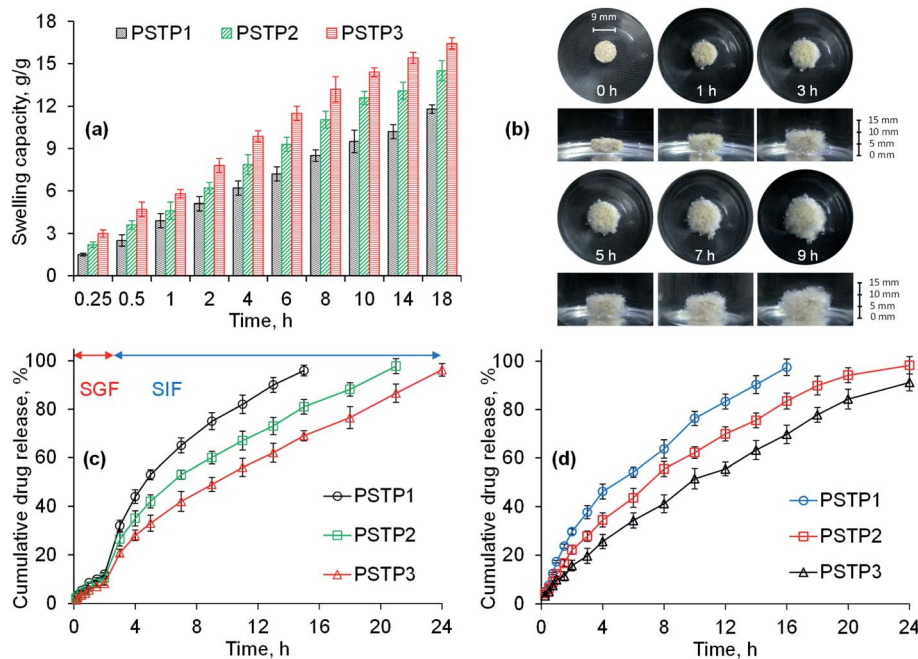


Fig. 6 Swelling capacity of PSTP3 in DW (a), photographs showing swelling response (aerial and axial view) of PSTP3 formulation in DW (b), the TP release study from PSH matrix tablets in SGF and SIF (c) and at pH 6.8 (d).

polymeric matrix, which leads to hydration and swelling of polymers, dissolves the drug, and brings about relaxation of polymer chains.<sup>50,51</sup> Consequently, the drug diffuses out of the matrix. Therefore, among various key factors upon which drug release from a water-swellable polymeric matrix depends, the swelling ability of the hydrogel in the dissolution media, the solubility of the drug in the dissolution media and interaction between the hydrogel and drug are important ones. TP was selected to assess the sustained release behavior of PSH due to its solubility over wide range of pH.

Owing to low swelling of PSH in an acidic environment, the release of TP in SGF was found to be insignificant (12, 10.5 and 8.2%) for PSTP1, PSTP2 and PSTP3, respectively, during 2 h study. Whereas, in SIF, due to the basic environment, the swelling capacity of PSH increases, which results in the increase of TP release and is noted to be more significant (98.85, 88.2 and 73.5%) for PSTP1, PSTP2 and PSTP3, respectively, after 16 h. Maximum drug release from PSTP1 (96%), PSTP2 (97.8%) and PSTP3 (96.3%) was observed after 15, 21 and 24 h, respectively. Moreover, it was also observed that as the concentration of PSH was increased, *i.e.*, PSTP3, the release of the drug decreased (Fig. 6c). Similar drug-release behavior was observed at pH 6.8 during the 24 h study (Fig. 6d). A more sustained or prolonged drug release profile was noted as the concentration of PSH was increased in the tablets. Therefore, it can be concluded that the drug release can be adjusted by increasing or decreasing the concentration of PSH in the tablets.

The release of a drug from a polymeric system is controlled by diffusion, swelling and erosion mechanism.<sup>36,37</sup> Drug-release mechanism was determined through Korsmeyer and Peppas model. The value of *n* determined the drug-release mechanism and its value for all formulations are expressed in Table 3. The

value of *n* for all three formulations was in the range of 0.616–0.729, which indicated that drug release followed the anomalous transport mechanism and both swelling of polymer and diffusion of the drug occurred simultaneously.<sup>36,37</sup>

### 3.12. Subacute toxicity studies

At the end of 28 days period of subacute toxicity studies, the animals from treated groups were found active and healthy. No behavioral changes were observed during the whole study period. Moreover, any other untoward effects, *i.e.*, allergy reactions, tremor, diarrhea, constipation and skin rashes were not observed, which demonstrated the nontoxic nature of PSH.

Table 3 Data of different drug release kinetics models

		PSTP1	PSTP2	PSTP3
Zero order	$R^2$	0.8664	0.9224	0.9576
	$K_0$	7.478	5.630	4.330
	MSC	1.8593	2.4225	3.0421
First order	$R^2$	0.9887	0.9935	0.9881
	$K_1$	0.148	0.105	0.076
	MSC	4.3261	4.8991	4.3171
Hixson–Crowell	$R^2$	0.9754	0.9893	0.9454
	$K_{HC}$	0.041	0.029	16.791
	MSC	3.5493	4.4073	2.7902
Higuchi	$R^2$	0.9720	0.9638	0.9937
	$K_H$	22.939	19.547	0.021
	MSC	3.4200	3.1867	4.9572
Korsmeyer–Peppas	$R^2$	0.9938	0.9981	0.9984
	$K_{KP}$	18.080	13.312	9.254
	MSC	4.7796	5.9864	6.1871
	<i>n</i>	0.616	0.664	0.729



Food intake in the animals from all treated groups was decreased during the whole study period (Table S1, see ESI†). The presence of swellable material in GIT may cause the delay empty time of the whole tract, which reduces appetite, resulting in less food intake and weight loss. No significant difference was observed in the body weight, the amount of water consumed and food intake by the treated and untreated animals during the whole study period. However, on days 21 and 28, a significant difference in the body weight of the animals from groups III and IV was noted. After prolonged consumption of PSH, the desirability or craving of taking food was reduced, which ultimately affect the body weight of the animals. Similarly, on day 28, a significant difference in food intake of the animals of group III and IV was also witnessed. The values of the absolute organ weights of the rats were recorded (Table S2, see ESI†) and they showed an insignificant difference in comparison to the control.

The hematological and biochemical parameters of the rats were found in the normal ranges and comparable to the control group animals (Table 4). An insignificant difference was observed in the values of complete blood count, liver function test, renal function test, erythrocyte sedimentation rate and serum electrolytes. However, a significant difference in the values of cholesterol, triglyceride and low-density lipoprotein (LDL) was observed in animals of group IV. Therefore, the daily intake of PSH can decrease the concentrations of cholesterol, triglyceride and LDL, which lead to a decrease in the risk of cardiovascular diseases.

### 3.13. Gross necropsy and histopathology

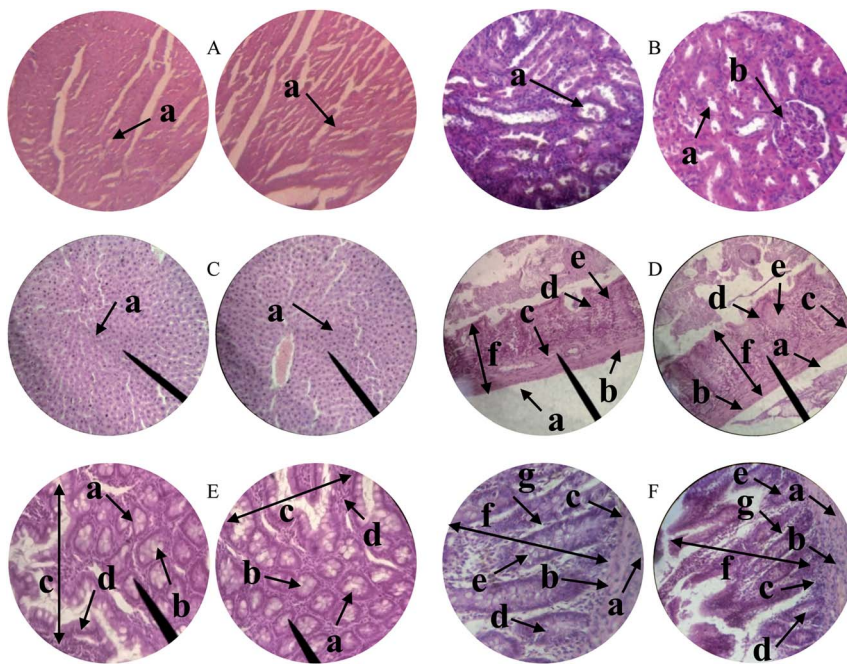
The possible toxic effects of PSH on the cellular architecture of the vital organs of the rats were evaluated through histopathology studies.<sup>52</sup> The results demonstrated that the tissues of

Table 4 Hematological and biochemical parameters of rats<sup>a</sup>

	Group I	Group II	Group III	Group IV
<b>CBC</b>				
TLC ( $10^3/\mu\text{L}^{-1}$ )	3.51 ± 1.01	3.33 ± 0.97	3.82 ± 1.13	3.91 ± 1.06
RBC ( $10^6/\mu\text{L}^{-1}$ )	8.11 ± 0.45	7.85 ± 0.32	8.01 ± 0.41	7.79 ± 0.29
Hb (g dL <sup>-1</sup> )	13.07 ± 0.68	13.3 ± 0.95	12.75 ± 0.78	13.11 ± 0.53
HCT (PCV) (%)	44.5 ± 3.8	41.6 ± 2.1	39.8 ± 4.1	40.9 ± 3.1
MCV (fL)	59.3 ± 4.1	60.9 ± 3.3	60.1 ± 3.8	61 ± 4.3
MCH (pg)	19.2 ± 1.7	20 ± 1.1	19.5 ± 1.5	21.1 ± 1.2
MCHC (g dL <sup>-1</sup> )	31.4 ± 0.94	30.7 ± 1.3	30.1 ± 1.1	29 ± 1.2
Platelet count ( $10^3/\mu\text{L}^{-1}$ )	571 ± 75.4	529 ± 65.3	512 ± 83.2	568 ± 95.2
Neutrophils (%)	22.5 ± 2.4	26.3 ± 3.1	24.8 ± 2.1	22.3 ± 2.7
Lymphocytes (%)	73.3 ± 4.5	69.3 ± 3.4	70.2 ± 4.1	73.4 ± 3.7
Monocytes (%)	2.1 ± 0.73	2.5 ± 0.91	2.8 ± 0.67	1.9 ± 1.1
Eosinophils (%)	1.1 ± 0.89	1.3 ± 0.11	1.5 ± 0.31	1.7 ± 0.29
<b>Lipid profile</b>				
Cholesterol (mg dL <sup>-1</sup> )	89 ± 7.1	81 ± 5.2	75 ± 5.9*	63 ± 5.8*
Triglyceride ( $\mu\text{mol L}^{-1}$ )	0.6 ± 0.09	0.5 ± 0.1	0.5 ± 0.05	0.4 ± 0.03*
HDL (mg dL <sup>-1</sup> )	28.1 ± 2.7	30 ± 3.7	32.4 ± 3.1	36.2 ± 4.1
LDL (mg dL <sup>-1</sup> )	42 ± 3.1	39 ± 2.8	35 ± 2.1	32 ± 3.3*
<b>Liver function test</b>				
Bilirubin (mg dL <sup>-1</sup> )	0.9 ± 0.2	1.4 ± 0.2	1.3 ± 0.1	1.1 ± 0.1
SGPT (ALT) (IU/L)	41 ± 4.5	53 ± 3.2	40 ± 4.1	46 ± 3.1
SGOT (AST) (IU/L)	77 ± 5.1	81 ± 6.1	72 ± 4.3	63 ± 3.8
ALP (IU/L)	98 ± 6.7	106 ± 7.1	114 ± 4.1	119 ± 7.3
Total protein (g dL <sup>-1</sup> )	6.2 ± 1.1	5.7 ± 0.9	5.1 ± 0.7	5.1 ± 0.9
Albumin (g dL <sup>-1</sup> )	3.9 ± 0.9	4.5 ± 1.3	4.3 ± 1.1	4.1 ± 1.5
Globulin (g dL <sup>-1</sup> )	1.6 ± 0.7	2.1 ± 0.7	1.9 ± 0.4	1.7 ± 0.8
A/G ratio	2.43 ± 0.85	2.14 ± 0.91	2.26 ± 0.78	2.41 ± 0.81
<b>Renal function test</b>				
Urea (mg dL <sup>-1</sup> )	55 ± 4.5	59 ± 6.7	47 ± 8.1	41 ± 4.7
Creatinine (mg dL <sup>-1</sup> )	0.6 ± 0.1	0.5 ± 0.1	0.9 ± 0.1	0.6 ± 0.2
<b>Hematology</b>				
ESR (mm h <sup>-1</sup> )	2.7 ± 0.7	3.1 ± 0.8	2.3 ± 0.3	3.3 ± 0.5
<b>Serum electrolyte</b>				
Potassium (mmol L <sup>-1</sup> )	5.1 ± 1.3	5.3 ± 0.6	5.9 ± 0.9	5.8 ± 1.5
Sodium (mmol L <sup>-1</sup> )	139 ± 8.1	142 ± 9.3	146 ± 5.5	140 ± 9.1

<sup>a</sup> Values expressed as mean ± SEM. \**p* < 0.05 compared with the control group.





**Fig. 7** Histopathology of the heart (A) depicting cardiac muscle fibers (a); kidney (B) showing renal tubules (a) and glomerulus (b); liver (C) showing plates of hepatocytes (a); gastric tissues (D) eliciting serosa (a) muscularis mucosae (b) submucosa (c) lamina propria (d) gastric glands (e) and mucosa (f); small intestine (E) depicting acinous lumen (a) columnar epithelial cell with basal nuclei (b) small intestinal villi (c) small intestinal villus (d) and colon (F) showing serosa (a), muscularis externa (b), submucosa (c), the lumen of crypt (d), colonic crypt (e), mucosa (f) and lamina propria (g).

vital organs did not show any change during histological examination of the heart, kidney, liver, gastric tissues, the small intestine and colon of treated rats (Fig. 7). Moreover, any sign of inflammation, necrosis, hemorrhage and lesion was not evident in the histology of all vital organs. Therefore, PSH can be administered for a long duration without any damage to the tissues of vital organs.

## 4. Conclusions

Alkali-extracted psyllium hydrogel (PSH) shows the pH-dependent swelling ability, *i.e.*, reasonably high swelling capacity in buffers of pH 6.8 and 7.4, and in deionized water, whereas insignificant swelling in the acidic buffer of pH 1.2. Moreover, the exceptional swelling and deswelling behavior of PSH against water and ethanol, water and normal saline and pH 7.4 and 1.2 environments indicated that PSH can be utilized as a potential candidate for site-specific and controlled drug delivery systems. The topographical analysis of PSH by SEM showed channeling in its surface, which is considered as one of the main reasons for its high swelling. The mechanism of TP release from PSH-based compressed tablets was found to be controlled by diffusion and swelling (non-Fickian). Prolong retention of PSH-based tablet formulations in simulated GIT environment (pH 6.8 and 7.4) established such a drug delivery system for sustained and targeted application/delivery of therapeutic agents. Subacute toxicity studies also proved the nontoxic nature of the PSH, which broadens its scope in the food and pharmaceutical industries. Because of the

extraordinary swelling capacity, admirable swelling and deswelling behavior, porous nature and sustained release potential, PSH may be recognized as a smart and intelligent material for pharmaceutical and biomedical applications.

## Author contributions

Conceptualization, supervision, project administration, M. A. H.; methodology, investigation, J. I. and A. A.; data curation, M. F. and T. T.; resources, S. Z. H. and I. H.; writing – original draft, J. I. and A. A.; writing – review & editing, M. T. H.

## Conflicts of interest

The authors declare that they have no conflict of interest.

## Acknowledgements

We are thankful to The University of Lahore (UOL) and University of Sargodha for providing the facilities for animal hosting and caring. Dr M. Zaman, Faculty of Pharmacy, UOL, Pakistan is also acknowledged for helpful discussion.

## References

- 1 R. Mohammadinejad, S. Karimi, S. Iravani and R. S. Varma, *Green Chem.*, 2016, **18**, 20–52.
- 2 L. Kokoska, P. Kloucek, O. Leuner and P. Novy, *Curr. Med. Chem.*, 2019, **26**, 5501–5541.





- 3 M. Kostag, K. Jedvert and O. A. El Seoud, *Int. J. Biol. Macromol.*, 2021, **167**, 687–718.
- 4 A. G. Atanasov, B. Waltenberger, E. M. Pferschy-Wenzig, T. Linder, C. Wawrosch, P. Uhrin, V. Temml, L. Wang, S. Schwaiger, E. H. Heiss, J. M. Rollinger, D. Schuster, J. M. Breuss, V. Bochkov, M. D. Mihovilovic, B. Kopp, R. Bauer, V. M. Dirsch and H. Stuppner, *Biotechnol. Adv.*, 2015, **33**, 1582–1614.
- 5 A. H. Blaesi and N. Saka, *Mater. Sci. Eng., C*, 2021, **120**, 110144.
- 6 A. W. Anderson, P. Baird, R. H. Davis Jr, S. Ferreri, M. Knudtson, A. Koraym, V. Waters and C. L. Williams, *Nutr. Rev.*, 2009, **67**, 188–205.
- 7 Y. Sun, L. Cheng, X. Zeng, X. Zhang, Y. Liu, Z. Wu and P. Weng, *Int. J. Biol. Macromol.*, 2021, **170**, 336–342.
- 8 M. S. Desai, A. M. Seekatz, N. M. Koropatkin, N. Kamada, C. A. Hickey, M. Wolter, N. A. Pudlo, S. Kitamoto, N. Terrapon, A. Muller, V. B. Young, B. Henrissat, P. Wilmes, T. S. Stappenbeck, G. Núñez and E. C. Martens, *Cell*, 2016, **167**, 1339–1353.
- 9 C. Soukoulis, C. Gaiani and L. Hoffmann, *Curr. Opin. Food Sci.*, 2018, **22**, 28–42.
- 10 M. A. Hussain, G. Muhammad, M. T. Haseeb and M. N. Tahir, Quince seed mucilage: a stimuli-responsive/smart biopolymer, in *Functional Biopolymers. Polymers and Polymeric Composites: A Reference Series*, ed. Jafar Mazumder M., Sheardown H. and Al-Ahmed A., Springer, Cham, Switzerland, 2019, pp. 127–148.
- 11 M. Farid-ul-Haq, M. T. Haseeb, M. A. Hussain, M. U. Ashraf, M. Naeem-ul-Hassan, S. Z. Hussain and I. Hussain, *J. Drug Delivery Sci. Technol.*, 2020, **58**, 101795.
- 12 J. Kuang, K. Y. Yuk and Y. K. M. Huh, *Carbohydr. Polym.*, 2011, **83**, 284–290.
- 13 Y. J. Kim and Y. T. Matsunaga, *J. Mater. Chem. B*, 2017, **5**, 4307–4321.
- 14 F. Chen, Y. Ren, J. Guo and F. Yan, *Chem. Commun.*, 2017, **53**, 1595–1598.
- 15 G. Muhammad, M. T. Haseeb, M. A. Hussain, M. U. Ashraf, M. Farid-ul-Haq and M. Zaman, *Drug Dev. Ind. Pharm.*, 2020, **46**, 122–134.
- 16 D. Schmaljohann, *Adv. Drug Delivery Rev.*, 2006, **58**, 1655–1670.
- 17 I. Gholamali, *Regener. Eng. Transl. Med.*, 2021, **7**, 91–114.
- 18 A. B. Samuelsen, I. Lund, J. M. Djahromi, B. S. Paulsen, L. K. Wold and S. H. Knutsen, *Carbohydr. Polym.*, 1999, **38**, 133–143.
- 19 M. A. Hussain, G. Muhammad, I. Jantan and S. N. A. Bukhari, *Polym. Rev.*, 2016, **56**, 1–30.
- 20 M. Bouchoucha, A. Faye, B. Savarieau and M. Arsac, *Gastroenterol. Clin. Biol.*, 2004, **28**, 438–443.
- 21 N. Washington, M. Harris, A. Mussellwhite and R. C. Spiller, *Am. J. Clin. Nutr.*, 1998, **67**, 317–321.
- 22 F. Fernandez-Banares, J. Hinojosa, J. L. Sanchez-Lombrana, E. Navarro, J. F. Martinez-Salmeron, A. Garcia-Puges, F. Gonzalez-Huix, J. Riera, V. Gonzalez-Lara, F. Dominguez-Abascal, J. J. Gine, J. Moles, F. Gomollon and M. A. Gassull, *Am. J. Gastroenterol.*, 1999, **94**, 427–433.
- 23 A. E. Moreyra, A. C. Wilson and A. Koraym, *Arch. Intern. Med.*, 2005, **165**, 1161–1166.
- 24 M. Sierra, J. J. Garcia, N. Fernandez, M. J. Diez and A. P. Calle, *Eur. J. Clin. Nutr.*, 2002, **56**, 830–842.
- 25 Z. Wei, H. Wang, X. Chen, B. Wang, Z. Rong, B. Wang, B. Su and H. Chen, *Eur. J. Clin. Nutr.*, 2009, **63**, 821–827.
- 26 M. Elli, D. Cattivelli, S. Soldi, M. Bonatti and L. Morelli, *J. Clin. Gastroenterol.*, 2008, **42**, S174–S176.
- 27 M. S. Izydorczyk and C. G. Biliaderis, *Carbohydr. Polym.*, 1995, **28**, 33–48.
- 28 M. S. Iqbal, J. Akbar, M. A. Hussain, S. Saghir and M. Sher, *Carbohydr. Polym.*, 2011, **83**, 1218–1225.
- 29 V. K. Thakur and M. K. Thakur, *J. Cleaner Prod.*, 2014, **82**, 1–15.
- 30 S. Saghir, M. S. Iqbal, M. A. Hussain, A. Koschella and T. Heinze, *Carbohydr. Polym.*, 2008, **74**, 309–317.
- 31 L. Lachmann, H. A. Liberman and J. L. Kanig, *Theory and Practice of Industrial Pharmacy*, Lea and Febiger, Philadelphia, 3rd edn, 1987.
- 32 S. Mirdarikvande, H. Sadeghi, A. Godarzi, M. Alahyari, H. Shasavari and F. Khani, *Biosci. Biotechnol. Res. Asia*, 2014, **11**, 205–209.
- 33 M. A. Hussain, L. Kiran, M. T. Haseeb, I. Hussain and S. Z. Hussain, *J. Polym. Res.*, 2020, **27**, 49.
- 34 E. Diez-Pena, I. Quijada-Garrido and J. M. Barrales-Rienda, *Polymer*, 2002, **43**, 4341–4348.
- 35 Y. Zhao, W. Chen, Y. Yang, X. Yang and H. Xu, *Colloid Polym. Sci.*, 2007, **285**, 1395–1400.
- 36 R. W. Korsmeyer, R. Gurny, E. M. Doelker, P. L. Buri and N. A. Peppas, *Int. J. Pharm.*, 1983, **15**, 25–35.
- 37 P. I. Ritger and N. A. Peppas, *J. Controlled Release*, 1987, **37**, 37–42.
- 38 J. Siepmann and N. A. Peppas, *Adv. Drug Delivery Rev.*, 2001, **48**, 139–157.
- 39 *OECD Guidelines for the Testing of Chemicals, Repeated Dose 28-day Oral Toxicity Study in Rodents*, OECD Test Guideline 407, ed. OECD, Paris, 2008.
- 40 G. K. Traesel, J. C. de Souza, A. L. de Barros, M. A. Souza, W. O. Schmitz, R. M. Muzzi, S. A. Oesterreich and A. C. Arena, *Food Chem. Toxicol.*, 2014, **74**, 320–325.
- 41 L. C. Cunha, F. S. Azeredo, A. C. V. Mendonça, M. S. Vieira, L. L. Pucci, M. C. Valadares, H. O. G. Freitas, A. A. S. Sena and R. S. L. Junior, *Rev. Bras. Farmacogn.*, 2009, **19**, 403–411.
- 42 M. Bhatia and M. Ahuja, *Int. J. Biol. Macromol.*, 2015, **72**, 495–501.
- 43 M. T. Haseeb, M. A. Hussain, S. H. Yuk, S. Bashir and M. Nauman, *Carbohydr. Polym.*, 2016, **136**, 750–756.
- 44 G. Muhammad, M. A. Hussain, M. U. Ashraf, M. T. Haseeb, S. Z. Hussain and I. Hussain, *RSC Adv.*, 2016, **6**, 23310–23317.
- 45 M. U. Ashraf, M. A. Hussain, G. Muhammad, M. T. Haseeb, S. Bashir, S. Z. Hussain and I. Hussain, *Int. J. Biol. Macromol.*, 2017, **95**, 138–144.
- 46 M. Farid-ul-Haq, M. A. Hussain, M. T. Haseeb, M. U. Ashraf, S. Z. Hussain and I. Hussain, *RSC Adv.*, 2020, **10**, 19832–19843.

47 C. Y. Tang and H. C. Allen, *J. Phys. Chem. A*, 2009, **113**, 7383–7393.

48 E. S. Dragan and D. F. Apopei, *Carbohydr. Polym.*, 2013, **92**, 23–32.

49 P. Patel, A. Mandal, V. Gote, D. Pal and A. K. Mitra, *J. Polym. Res.*, 2019, **26**, 131.

50 S. Dogu, M. Kilic and O. Okay, *J. Appl. Polym. Sci.*, 2009, **113**, 1375–1382.

51 A. Razmjou, G. P. Simon and H. Wang, *Chem. Eng. J.*, 2013, **215–216**, 913–920.

52 B. A. Lodhi, M. A. Hussain, M. U. Ashraf, M. Farid-ul-Haq, M. T. Haseeb and T. Tabassum, *Cellul. Chem. Technol.*, 2020, **54**, 291–299.

